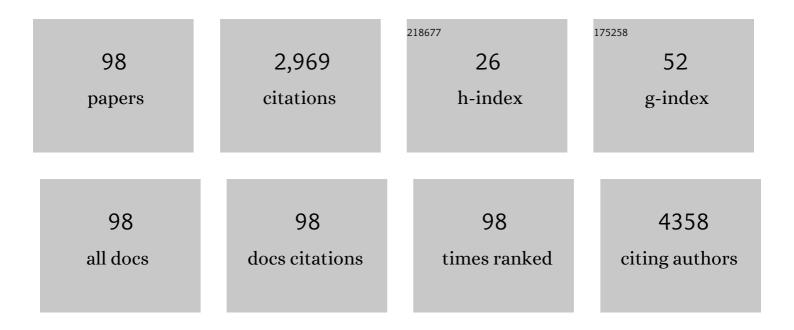
A Michael Peters

List of Publications by Year in descending order

Source: https://exaly.com/author-pdf/4609021/publications.pdf Version: 2024-02-01



#	Article	IF	CITATIONS
1	Gamma camera imaging in hepatobiliary diseases. , 2022, , .		0
2	Gamma camera imaging of the kidney. , 2022, , .		1
3	Measurement of Eosinophil Kinetics In Vivo. Methods in Molecular Biology, 2021, 2241, 183-191.	0.9	0
4	82 Rb tissue kinetics in humans. Clinical Physiology and Functional Imaging, 2021, 41, 245-252.	1.2	0
5	Measuring myocardial blood flow with 82rubidium using Gjedde–Patlak–Rutland graphical analysis. Annals of Nuclear Medicine, 2021, 35, 777-784.	2.2	0
6	Estimated glomerular filtration rate equations in people of self-reported black ethnicity in the United Kingdom: Inappropriate adjustment for ethnicity may lead to reduced access to care. PLoS ONE, 2021, 16, e0255869.	2.5	29
7	"Latent―and "constitutional―lymphedema, useful terms to complement the terms "primary―and "secondary―lymphedema. Journal of Vascular Surgery: Venous and Lymphatic Disorders, 2021, 9, 1089-1092.	1.6	5
8	Hepatic bile acid transport increases in the postprandial state: A functional 11C-CSar PET/CT study in healthy humans. JHEP Reports, 2021, 3, 100357.	4.9	1
9	New gender-specific formulae for estimating extracellular fluid volume from height and weight in adults. Nuclear Medicine Communications, 2021, 42, 58-62.	1.1	0
10	Hepatic and splenic ¹⁸ Fâ€FDG blood clearance rates (Ki) in hepatic steatosis and diabetes mellitus. Clinical Physiology and Functional Imaging, 2020, 40, 99-105.	1.2	3
11	Bronchopulmonary MDR protein expression may protect against COVID-19 infection. Nuclear Medicine Communications, 2020, 41, 1107-1108.	1.1	0
12	Stimulation of the hepatic arterial buffer response using exogenous adenosine: hepatic rest/stress perfusion imaging. European Radiology, 2020, 30, 5852-5861.	4.5	11
13	Lesson of the month: novel method to quantify neutrophil uptake in early lung cancer using SPECT-CT. Thorax, 2020, 75, 1020-1023.	5.6	5
14	Absence of hepatic activity in lymphoscintigraphy performed with Tc-99m-Nanoscan. Nuclear Medicine Communications, 2020, 41, 505-509.	1.1	1
15	FDG PET/CT of the nonâ€malignant liver in an increasingly obese world population. Clinical Physiology and Functional Imaging, 2020, 40, 304-319.	1.2	17
16	Whole-body 75SeHCAT retention is determined by entero-hepatic bile acid recycling rate. Nuclear Medicine Communications, 2020, 41, 750-752.	1.1	0
17	Use of autologous ^{99m} Technetium-labelled neutrophils to quantify lung neutrophil clearance in COPD. Thorax, 2019, 74, 659-666.	5.6	21
18	Lung clearance of inhaled aerosol of Tcâ€99mâ€methoxyisobutyl isonitrile: relationships with cigarette smoking, age and gender. Clinical Physiology and Functional Imaging, 2019, 39, 236-239.	1.2	6

#	Article	IF	CITATIONS
19	The appropriate whole body metric for calculating standardised uptake value and the influence of sex. Nuclear Medicine Communications, 2019, 40, 3-7.	1.1	7
20	Relationship between regional hepatic glucose metabolism and regional distribution of hepatic fat. Nuclear Medicine Communications, 2019, 40, 212-218.	1.1	4
21	Tissue standardized uptake value is a closer surrogate of blood fluorine-18 fluorodeoxyglucose clearance after division by blood standardized uptake value, illustrated in brain and liver. Nuclear Medicine Communications, 2019, 40, 552-554.	1.1	4
22	Intrahepatic fluorine-18-fluorodeoxyglucose kinetics measured by least squares nonlinear computer modelling and Gjedde–Patlak–Rutland graphical analysis. Nuclear Medicine Communications, 2019, 40, 675-683.	1.1	4
23	Reply. Journal of Allergy and Clinical Immunology, 2019, 143, 1265-1266.	2.9	0
24	Effect of blood glucose level on standardized uptake value (SUV) in 18F- FDG PET-scan: a systematic review and meta-analysis of 20,807 individual SUV measurements. European Journal of Nuclear Medicine and Molecular Imaging, 2019, 46, 224-237.	6.4	66
25	<i>In vivo</i> imaging of hepatic neutrophil migration in severe alcoholic hepatitis with 111In-radiolabelled leucocytes. Bioscience Reports, 2018, 38, .	2.4	6
26	The precise physiological definition of tissue perfusion and clearance measured from imaging. European Journal of Nuclear Medicine and Molecular Imaging, 2018, 45, 1139-1141.	6.4	7
27	Vascular inflammation and metabolic activity in hematopoietic organs and liver in familial combined hyperlipidemia and heterozygous familial hypercholesterolemia. Journal of Clinical Lipidology, 2018, 12, 33-43.	1.5	19
28	Lymphatic drainage efficiency: a new parameter of lymphatic function. Acta Radiologica, 2018, 59, 1097-1101.	1.1	7
29	Glomerular filtration rate: new age- and gender- specific reference ranges and thresholds for living kidney donation. BMC Nephrology, 2018, 19, 336.	1.8	51
30	InÂvivo imaging reveals increased eosinophil uptake in the lungs of obese asthmatic patients. Journal of Allergy and Clinical Immunology, 2018, 142, 1659-1662.e8.	2.9	30
31	Radiolabelled leucocytes in human pulmonary disease. British Medical Bulletin, 2018, 127, 69-82.	6.9	4
32	Assessment of alteration in liver 18F–FDG uptake due to steatosis in lymphoma patients and its impact on the Deauville score. European Journal of Nuclear Medicine and Molecular Imaging, 2018, 45, 2231-2232.	6.4	1
33	The extent to which standardized uptake values reflect FDG phosphorylation in the liver and spleen as functions of time after injection of 18F-fluorodeoxyglucose. EJNMMI Research, 2017, 7, 13.	2.5	12
34	New exponential functions based on CT density to estimate the percentage of liver that is fat. British Journal of Radiology, 2017, 90, 20170186.	2.2	3
35	The cardiosplenic axis. Nuclear Medicine Communications, 2017, 38, 205-208.	1.1	6
36	Fasting hepatic glucose uptake is higher in men than women. Physiological Reports, 2017, 5, e13174.	1.7	14

#	Article	IF	CITATIONS
37	Importance of accurate ilio-inguinal quantification in lower extremity lymphoscintigraphy. Nuclear Medicine Communications, 2017, 38, 209-214.	1.1	12
38	Effects of tocilizumab on neutrophil function and kinetics. European Journal of Clinical Investigation, 2017, 47, 736-745.	3.4	44
39	Circulating granulocyte lifespan in compensated alcohol-related cirrhosis: a pilot study. Physiological Reports, 2016, 4, e12836.	1.7	2
40	Scaling of Glomerular Filtration Rate and SUV for Body Size: The Curious Conflict of Whole-Body Metric Preferences. Journal of Nuclear Medicine, 2016, 57, 2028-2028.	5.0	3
41	Heterogeneity of intrahepatic fat distribution determined by 18F-FDG PET and CT. Annals of Nuclear Medicine, 2016, 30, 200-206.	2.2	9
42	Does the Clearance of Inhaled ^{99m} Tc-Sestamibi Correlate with Multidrug Resistance Protein 1 Expression in the Human Lung?. Radiology, 2016, 280, 924-930.	7.3	10
43	Constitutively Enhanced Lymphatic Pumping in the Upper Limbs of Women Who Later Develop Breast Cancer-Related Lymphedema. Lymphatic Research and Biology, 2016, 14, 50-61.	1.1	38
44	Reproducible lymph-to-blood transfer of Tc-99m-nanocolloid in a patient with abnormal lymphatic function. Vascular Medicine, 2015, 20, 569-570.	1.5	0
45	Quantification of tumour 18 F-FDG uptake: Normalise to blood glucose or scale to liver uptake?. European Radiology, 2015, 25, 2701-2708.	4.5	35
46	Fallacy of Quantifying Lymphoma Activity by Scaling to the Liver in [¹⁸ F]Fluorodeoxyglucose Positron Emission Tomography (Deauville criteria). Journal of Clinical Oncology, 2015, 33, 4120-4121.	1.6	3
47	Evaluation of non-polynomial equations for one-compartment correction of slope-intercept GFR: Theoretical prediction and experimental measurement. Scandinavian Journal of Clinical and Laboratory Investigation, 2014, 74, 611-619.	1.2	0
48	Biomarkers of eosinophilic inflammation in asthma. Expert Review of Respiratory Medicine, 2014, 8, 143-150.	2.5	23
49	Mathematical modeling supports the presence of neutrophil depriming in vivo. Physiological Reports, 2014, 2, e00241.	1.7	15
50	Accumulation of ¹⁸ F-FDG in the Liver in Hepatic Steatosis. American Journal of Roentgenology, 2014, 203, 643-648.	2.2	52
51	Old tracer for a new purpose. Nuclear Medicine Communications, 2014, 35, 1058-1066.	1.1	1
52	Hepatic steatosis is associated with increased hepatic FDG uptake. European Journal of Radiology, 2014, 83, 751-755.	2.6	37
53	Recycling rate of bile acids in the enterohepatic recirculation as a major determinant of whole body 75SeHCAT retention. European Journal of Nuclear Medicine and Molecular Imaging, 2013, 40, 1618-1621.	6.4	14
54	Assessment of Glomerular Filtration Rate Measurement with Plasma Sampling: A Technical Review. Journal of Nuclear Medicine Technology, 2013, 41, 67-75.	0.8	45

#	Article	IF	CITATIONS
55	Higher extracellular fluid volume in women is concealed by scaling to body surface area. Scandinavian Journal of Clinical and Laboratory Investigation, 2013, 73, 546-552.	1.2	6
56	Association between bile acid turnover and osteoporosis in postmenopausal women. Nuclear Medicine Communications, 2013, 34, 597-600.	1.1	19
57	Extracellular fluid volume and glomerular filtration rate in 1878 healthy potential renal transplant donors: effects of age, gender, obesity and scaling. Nephrology Dialysis Transplantation, 2012, 27, 1429-1437.	0.7	51
58	Use of 111-Indium–labeled autologous eosinophils to establish the in vivo kinetics of human eosinophils in healthy subjects. Blood, 2012, 120, 4068-4071.	1.4	58
59	Acute lung injury results from failure of neutrophil deâ€priming: a new hypothesis. European Journal of Clinical Investigation, 2012, 42, 1342-1349.	3.4	31
60	Why the spleen is a very rare site for metastases from epithelial cancers. Medical Hypotheses, 2012, 78, 26-28.	1.5	12
61	The reliability of glomerular filtration rate measured from plasma clearance: a multi-centre study of 1,878 healthy potential renal transplant donors. European Journal of Nuclear Medicine and Molecular Imaging, 2012, 39, 715-722.	6.4	13
62	Estimation of extracellular fluid volume in children. Pediatric Nephrology, 2012, 27, 1149-1155.	1.7	1
63	Re-evaluation of the new Jodal–Brochner-Mortensen equation for one-pool correction of slope–intercept measurement of glomerular filtration rate. Nuclear Medicine Communications, 2011, 32, 375-380.	1.1	8
64	Extracellular fluid volume and glomerular filtration rate. Nuclear Medicine Communications, 2011, 32, 649-653.	1.1	15
65	Measuring wholeâ€body neutrophil redistribution using a dedicated wholeâ€body counter and ultraâ€ŀow doses of ¹¹¹ Indium. European Journal of Clinical Investigation, 2011, 41, 77-83.	3.4	12
66	Quantification of neutrophil migration into the lungs of patients with chronic obstructive pulmonary disease. European Journal of Nuclear Medicine and Molecular Imaging, 2011, 38, 911-919.	6.4	23
67	Popliteal Node Visualization During Standard Pedal Lymphoscintigraphy for a Swollen Limb Indicates Impaired Lymph Drainage. American Journal of Roentgenology, 2011, 197, 1443-1448.	2.2	32
68	Slope-only glomerular filtration rate and single-sample glomerular filtration rate as measurements of the ratio of glomerular filtration rate to extracellular fluid volume. Nephrology, 2010, 15, 281-287.	1.6	3
69	Estimated Lean Body Mass Is More Appropriate than Body Surface Area for Scaling Glomerular Filtration Rate and Extracellular Fluid Volume. Nephron Clinical Practice, 2010, 116, c75-c80.	2.3	29
70	Measurement of lymph node function from the extraction of immunoglobulin in lymph. Scandinavian Journal of Clinical and Laboratory Investigation, 2010, 70, 112-115.	1.2	5
71	Use of Body Surface Area for Assessing Extracellular Fluid Volume and Glomerular Filtration Rate in Obesity. American Journal of Nephrology, 2010, 31, 209-213.	3.1	12
72	Neutrophil kinetics in health and disease. Trends in Immunology, 2010, 31, 318-324.	6.8	875

#	Article	IF	CITATIONS
73	Extracellular fluid volume in patients with cancer. Nuclear Medicine Communications, 2010, 31, 359-365.	1.1	3
74	Functional Variation in Lymph Node Arrangements within the Axilla. Lymphatic Research and Biology, 2009, 7, 139-144.	1.1	6
75	Accurate measurement of extracellular fluid volume from the slope/intercept technique after bolus injection of a filtration marker. Physiological Measurement, 2009, 30, 1371-1379.	2.1	23
76	Evaluation of the Modification of Diet in Renal Disease equation (eGFR) against simultaneous, dual-marker multi-sample measurements of glomerular filtration rate. Annals of Clinical Biochemistry, 2009, 46, 58-64.	1.6	7
77	Comparison of GFR Measurements Assessed From Single Versus Multiple Samples. American Journal of Kidney Diseases, 2009, 54, 278-288.	1.9	42
78	Does P-glycoprotein have a role in the lung clearances of inhaled 99mTc-sestamibi and 99mTc-tetrofosmin?. Nuclear Medicine Communications, 2009, 30, 617-621.	1.1	3
79	Pulmonary elimination rate of inhaled99mTc-sestamibi radioaerosol is delayed in healthy cigarette smokers. British Journal of Clinical Pharmacology, 2008, 65, 611-614.	2.4	19
80	Suitability of a simplified technique based on iohexol for decentralized measurement of glomerular filtration rate. Scandinavian Journal of Urology and Nephrology, 2008, 42, 472-480.	1.4	16
81	Reproducibilities and responses to food intake of GFR measured with chromium-51-EDTA and iohexol simultaneously and independently in normal subjects. Nephrology Dialysis Transplantation, 2008, 23, 1902-1909.	0.7	31
82	Clinical governance improves the quality of nuclear medicine reporting. Nuclear Medicine Communications, 2008, 29, 999-1001.	1.1	7
83	Using the slope-only technique and estimated glomerular filtration rate for checking the reliability of slope-intercept measurement of glomerular filtration rate. Nuclear Medicine Communications, 2008, 29, 1086-1092.	1.1	10
84	Comparison between slope–intercept and slope-only techniques for measuring glomerular filtration rate: Use of two independent markers and an independent arbiter. Nuclear Medicine Communications, 2007, 28, 711-718.	1.1	6
85	Imaging of Lymphatic Vessels in Breast Cancer–Related Lymphedema: Intradermal Versus Subcutaneous Injection of99mTc-Immunoglobulin. American Journal of Roentgenology, 2006, 186, 1349-1355.	2.2	29
86	Quantification of disease activity in patients undergoing leucocyte scintigraphy for suspected inflammatory bowel disease. European Journal of Nuclear Medicine and Molecular Imaging, 2005, 32, 329-337.	6.4	10
87	Regional Distribution of Epifascial Swelling and Epifascial Lymph Drainage Rate Constants in Breast Cancer-Related Lymphedema. Lymphatic Research and Biology, 2005, 3, 3-15.	1.1	40
88	Measurement of the extraction fractions of nanocolloid and polyclonal immunoglobulin by axillary lymph nodes in patients with breast cancer. Nuclear Medicine Communications, 2004, 25, 935-940.	1.1	13
89	Clinical audit in nuclear medicine. Nuclear Medicine Communications, 2004, 25, 97-103.	1.1	13
90	Physiologic granulocyte destruction in vivo by apoptosis. Journal of Nuclear Medicine, 2004, 45, 526.	5.0	2

#	Article	IF	CITATIONS
91	Indexing glomerular filtration rate to suit children. Journal of Nuclear Medicine, 2003, 44, 1037-43.	5.0	43
92	Defective Fc-dependent processing of immune complexes in patients with systemic lupus erythematosus. Arthritis and Rheumatism, 2002, 46, 1028-1038.	6.7	50
93	Reduction of chemokine levels and leukocyte traffic to joints by tumor necrosis factor α blockade in patients with rheumatoid arthritis. Arthritis and Rheumatism, 2000, 43, 38-47.	6.7	378
94	ECAT ART — a continuously rotating PET camera: Performance characteristics, initial clinical studies, and installation considerations in a nuclear medicine department. European Journal of Nuclear Medicine and Molecular Imaging, 1997, 24, 6-15.	2.1	80
95	Pulmonary technetium-99m diethylene triamine penta-acetic acid aerosol clearance as an index of lung injury. European Journal of Nuclear Medicine and Molecular Imaging, 1997, 24, 81-87.	2.1	60
96	Endothelial activation in monosodium urate monohydrate crystal-induced inflammation. In vitro and in vivo studies on the roles of tumor necrosis factor α and interleukin-1. Arthritis and Rheumatism, 1997, 40, 955-965.	6.7	91
97	Use of a radiolabeled monoclonal antibody against e-selectin for imaging of endothelial activation in rheumatoid arthritis. Arthritis and Rheumatism, 1996, 39, 1371-1375.	6.7	94
98	Lung Scintigraphy. , 0, , 135-169.		0

98 Lung Scintigraphy. , 0, , 135-169.

0